Chapter 2
Experimental Apparatuses and Measurements

Abstract In order to study the interactions between flexible plates and two-dimensional flow, a steady and uniform two-dimensional flow is required. In our studies, soap film tunnels are employed to provide such two-dimensional flow. The flow structure in the flow field is revealed by optical methods. In this chapter, the structure of soap film tunnels are introduced. All the experiments discussed in this thesis were carried out using these devices. Flow visualization method, the measurements of physical parameters and properties of the soap film and filaments are also introduced in this chapter.

2.1 Soap Film Tunnels

The first soap film device used in fluid experiment appeared in 1980s. After a rapid evolution that happened in 1990s, the designs of soap film tunnels became stable, controllable and repeatable. Rutgers et al. (2001) and Georgiev and Vorobieff (2002) introduced their designs of gravity-driven vertical and horizontal soap film tunnels in *Review of Scientific Instruments*. These two sorts of devices can make flowing soap film achieve different flow speed ranges. The designs are improved according to the situations we encountered in experiments. In this chapter, the designs of our vertical and horizontal soap film tunnels are introduced.

2.1.1 Vertical Soap Film Tunnel

A vertical soap film tunnel consists of an upper reservoir, a metal frame, a flow frame, a lower recycle reservoir, a pump, tubes, valves and pull strings. Figure 2.1 shows the schematic of the vertical soap film tunnel.

L. Jia, *The Interaction Between Flexible Plates and Fluid in Two-dimensional Flow*, Springer Theses, DOI: 10.1007/978-3-662-43675-2_2,

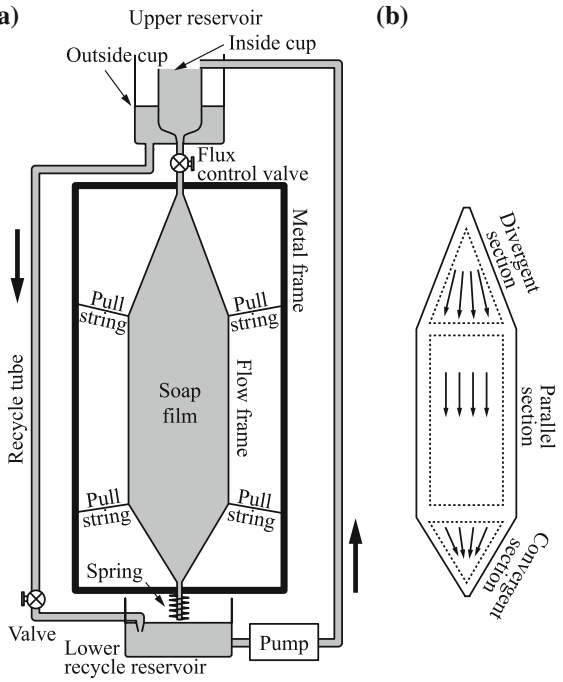

Fig. 2.1 Vertical soap film tunnel. Arrows indicate the flow direction. **a** Schematic of the vertical soap film tunnel. **b** Three sections of flow frame

The upper reservoir consists of two cups, a small cup inside a big one. In the experiments, a pump drives soap film solution into the inside cup of the upper reservoir. Once the inside cup is full, soap solution overflows to outside cup, and then flows back to the lower recycle reservoir through the recycle tube. This design keeps the water head of the inside cup constant, and guarantees the flux from the upper reservoir to the flow frame is steady. Corrosion–resistant material was used in manufacturing the upper reservoir to avoid any erosion damage from the soap solution. We made the upper reservoir with two sizes of Polyethylene Terephthalate (PET) bottles. They were bonding together with melt plastic. A tube is connected to the bottom of the insider cup of the upper reservoir. The soap solution in the inside cup flows to the flow frame through the tube. A valve is placed in the middle of the tube to control the flow flux.

Soap film is formed on the flow frame. The flow frame is connected to an outer metal frame with pull strings and spring. The flow frame is constituted by nylon threads. Two high-strength nylon fishing lines are set vertically in the metal frame, connecting the top centre and bottom centre of the frame. The diameter of the fishing line is 1 mm. The topper connection point between the nylon lines and the metal frame is also connected with the tube and flux control valve. The bottom connection point between the nylon lines and the metal frame is fitted in a spring. On each of the nylon lines, there are two additional pull strings. The pull strings are used to pull the nylon lines away from each other. When they are loose, two nylon lines stay

close to each other with the action of the spring. Once the strings are pulled tight, the spring contracts, and two nylon lines form a hexagon flow frame as shown in Fig. 2.1a. In the experiment preparation stage, the strings are released, and two nylon lines keep together. After opening the flow control valve, soap solution comes out of the upper reservoir, flows through the nylon lines, and finally reaches the lower recycle reservoir. Once the soap solution flows on the nylon lines, the strings are pulled aside. The elastic nylon lines become a hexagon flow frame. For the surface tension of the soap solution is small, a flowing soap film is formed on the flow frame.

The flow frame can be divided into three sections, a divergent section, a parallel section and a convergent section, as shown in Fig. 2.1b. After the soap solution flows out of the control valve nozzle, it flows into the divergent part of the hexagon frame. In the divergent section, two nylon lines keeps a certain expanding angle. Soap solution expands to soap film in this section. The soap film then flows into the parallel section of the hexagon frame. In this section, two nylon lines keeps parallel. Due to the gravity, the flow speed of the soap film accelerates at the top of this section. A stable flow speed is achieved once the air resistance and gravity come to a balance. The experiments can only be carried out in the middle part of this section, where the flow speed is stable. Soap film then flows into the convergent section, where it becomes soap solution again and flows into the lower recycle reservoir.

The lower recycle reservoir is located at the bottom of the tunnel. It collects all the soap solution coming from the outside cup of the upper reservoir and flow frame. The collected soap solution is then being pump into the upper reservoir again. In order to avoid the influence of vibration from the pump, the lower reservoir does not directly contact with the frame.

One thing should be noticed in the experiments is that the recycled soap solution usually contains bubbles of different sizes. Large bubbles do not affect the experiments for they just float on the solution surface. Small bubbles stay in soap solution. They are then pumped up into the upper reservoir, and flow through the control valve. At the narrow place in the valve, small bubbles accumulate to become a large bubble that blocks the flow. As a result, the flux is changed and the maintain time of soap film is shorten. Two major reasons are found to produce small bubbles. The first one is the water level of lower recycle reservoir. If the water level is too low to cover the pump, a small amount of air is sucked into the pump. The air becomes tiny bubbles with the blending of the pump blades. The other reason is that the flow speed is too high in the recycle tube. Due to the height difference, gravity drives the soap solution from the outside cup of the upper reservoir to run very fast back to the recycle reservoir through the recycle tube. However, the solution in the outside cup comes from the inside cup. Its flux is limited. As a result, the outside cup does not always contain soap solution. In the recycle tube, soap solution is isolated to be segments by air. The soap solution mixed with air flows into the recycle reservoir and produces a lot of bubbles. In order to solve the problem with bubbles, two strategies are taken. The first one is to get enough soap solution to cover the whole bump, or connect the pump inlet with the bottom of the recycle reservoir, to avoid the pump from sucking in air. The second one is to control the flux of the recycle tube with a valve. By controlling the flux of soap solution in the recycle tube, and making it equal to the

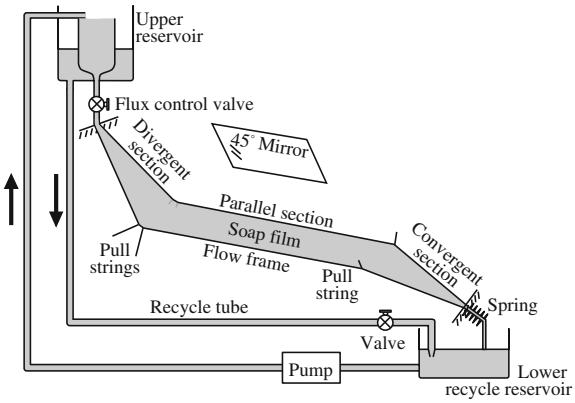

Fig. 2.2 Schematic of a horizontal soap film tunnel. Arrows indicate the flow direction

flux overflowing from the inside cup of the upper reservoir, air bubbles are avoid to be produced in the recycle tube.

2.1.2 Horizontal Soap Film Tunnel

The schematic of a horizontal soap film tunnel is shown in Fig. 2.2. The horizontal soap film tunnel also consists of an upper reservoir, a metal frame, a flow frame, and a lower recycle reservoir, a pump, tubes, valves and pull strings. The soap solution flows through the upper reservoir and flux control valve to the flow frame. Soap film forms and flows on the flow frame. And finally, the soap solution flows into the lower recycle reservoir. The flow frame is connected to the metal frame, which is omitted in the figure. Since the test section is horizontal in the horizontal soap film, a 45° mirror is located on the top of the test section for illumination and image recording.

Compared with the vertical soap film tunnel, the main difference between two devices in structure is the flow frame. In the horizontal soap film tunnel, the parallel section is no longer vertical. It is slightly inclined to horizon with an adjustable angle. This modification significantly decreases the component of gravity in the soap film flow direction. In order to make the soap film flow stable, the divergent and convergent sections are modified from vertical to inclined design.

In the design of the horizontal soap film tunnel, the divergent and parallel parts are no longer in the same plane. In order to make the soap film flows more stable at the joint of the divergent and parallel sections and avoid the formation of vortices at the connection corner, two more pull strings are added. The additional strings make the divergent and parallel sections connected more smoothly. Figure 2.3 shows the side views of the horizontal soap film tunnel at the joint. Figure 2.3a shows the flow frame with only one pull string on each nylon line, and Fig. 2.3b shows the flow frame with two strings on each nylon line. The highest place of the soap film is marked with thin white line in the figure. By using two pull string on each nylon line,

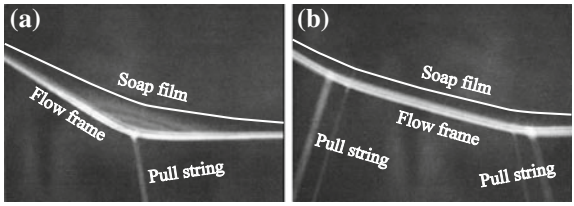

Fig. 2.3 Side views at the joint of the divergent and parallel sections in the horizontal soap film tunnel. Soap film, pull strings and flow frame are marked in the photos. **a** using one pull string. **b** using two pulling strings

the soap film is much closer to the flow frame. This modification makes the flow at the connection corner more stable, effectively avoiding the structure disturbances in the soap film.

2.2 Illumination Device

The change in soap film thickness can be revealed by Schlieren (Settles 2001, pp. 39–76), Shadowgraph (Settles 2001, pp. 143–164), and Interferometry (Greco and Molesini 1996). Interferometry is the most common method employed. Incident light is reflected from two liquid-air interfaces of the soap film. The thickness of the film is comparable with the incident light wavelength. As a result, the reflected light from two interfaces interferes and forms fringes. The interference fringes reflect the changes of the film thickness. Chomaz (2001) proved theoretically that the thickness of soap film is related to the pressure and vorticity fields under the condition that the flow velocity is much lower than the Marangoni elastic wave velocity of the soap film.

In order to visualize the flow structure clearly, monochromatic light source is preferred. Monochromatic light can reveal the thickness change of the soap film with clear interference fringes. Since the soap film is transparent, its reflectance is low. The brightness of the light source should be sufficient so that the interference fringes formed by the reflected light is strong enough to be recorded. And the luminous efficiency should also be considered. For the light source should not be damaged by overheated with a long-time working.

A sodium-vapour lamp features well monochromaticity, high brightness and good luminous efficiency. It is a gas-discharge lamp. The efficiency of sodium-vapour lamp is related to the sodium-vapour pressure. Two peaks exist at pressure of 0.5 and 10^4 Pa. Low pressure sodium lamp has higher efficient and better monochromaticity than high pressure sodium (HPS) lamp. But its power is much lower than HPS lamp and is not available in Hefei at the time the thesis project started. In our studies, HPS lamps are used in the light source. The HPS lamp works at 10^4 Pa. Figure 2.4 shows the circuit of the HPS lamp and its spectrum over time. When the lamp is working, two electrodes discharge through the high pressure sodium-vapour. Since the discharge current of sodium vapour is too large, mercury is added as buffer gas to increase the voltage gradient, and a ballast is used in circuit to limit the current

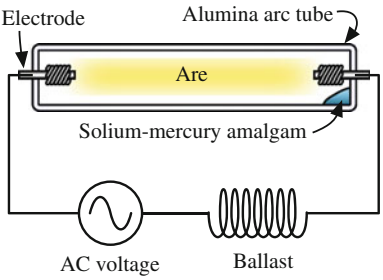

Fig. 2.4 Circuit diagram of a high pressure sodium lamp (Sakurambo 2006), licensed under the Creative Commons Attribution-Share Alike 3.0 Unported license.

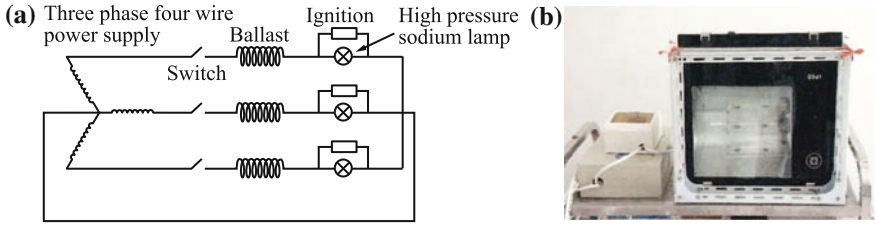

Fig. 2.5 Light source used in experiments. **a** The circuit of the light. **b** The device photo. The *big* box on the *left* side contains the ballasts and ignitions. The *small* box on it contains switches. The light is on the *right* side. Three HPS bulbs are used in the light. They are installed behind a heat resistance glass with a reflector on their back

as shown in Fig. 2.4. The spectrum and brightness of a HPS lamp change over time. When it is started, at the beginning, the lamp emits mainly D-line spectrum at around 589 nm. The brightness is low. With the increase of time, the brightness of the lamp is gradually increased, and the spectrum is gradually enriched. The interference fringes of wide spectrum are not as clear as monochromatic light. But at the time the lamp has just started, the brightness of the lamp is not enough to meet the requirement of a high speed camera to record the interference fringes. Thus in the experiments, the HPS lamp needs to be turned on for a while until the brightness is sufficient. The interference fringes recorded by cameras are mixed sodium yellow light with other spectrum.

The HPS lamp is a gas-discharge lamp. Its brightness is changing periodic with the AC voltage. As a result, a considerable numbers of the recorded images are underexposure, no matter the images are taken by single shot or continuous shooting. To overcome this defect, a light source with three HPS lamps was designed. These lamps are connected with different phases in three-phase four-wire power supply. The power supply phase difference between any two lamps is 120°. At any time, there is at least one lamp is light on to avoid the underexposure problem. Figure 2.5 shows the circuit design and the device photo.

2.3 Physical Properties of Soap Film

In this thesis, we use soap film to carry out two-dimensional experimental studies. The physical parameters of the flow field are needed to be measured. The measurement methods of soap film parameters are introduced in this section.

2.3.1 Viscosity

A soap film is comprised of two air–liquid surfactant layers and one intermediate soap solution layer. Its viscosity is consisted by these layers (Trapeznikov 1957) and written as,

$$\mu_f = \mu_b + 2\frac{\mu_s}{d_f}, \tag{2.1}$$

where μ_b is the viscosity of soap solution, μ_s is the viscosity of the surfactant, and d_f is the thickness of the soap film.

Martin and Wu (1995) proposed a direct measurement of the viscosity of a soap film. They placed a metal disc with a mass of only 0.08 g in a plastic ring. A glass fibre goes through a hole located at the centre of the metal disc. The fibre is fixed in the base. A horseshoe magnet is set on the base. When the measurement starts, a soap film is formed between the metal disc and outside plastic ring. Since the disc is light, it is suspended in the air. Turning the horseshoe magnet on the base, current is generated in the metal disc. According to the Lenz law, the metal disc will rotate with the magnet. By measuring the transient response or the steady stress–strain relationship of the disc, the corresponding soap film viscosity is calculated. This direct measurement method is accurate and reliable. But as shown in Eq. 2.1 shows, the viscosity of a soap film is related to its thickness. The thickness of soap film provided by the vertical and horizontal soap film tunnels is varying with flow speed. And the viscosity of soap film is related to ambient temperature, the ratio of surfactant to water, and many other factors. Any measurement in advance cannot accurately reflect the viscosity of the soap film in the experiments.

In this thesis, the viscosity of the soap film is calculated according to *Re*-*St* relationship. Here *Re* and *St* stand for Reynolds number and Strouhal number, respectively. In the studies of wake of a cylinder in a uniform flow, once the Reynolds number exceeds a certain value, Kármán Vortex Street is formed in the wake and flows downstream as shown in Fig. 2.6. The vortex shedding frequency is related to cylinder diameter, flow velocity and viscosity.

Strouhal number (St) characterizes the vibration in flow, and Reynolds number (Re) number characterizes the ratio of inertia force to viscous force. Further researches reveal the relationship between St and Re. Here St number is defined as,

$$St = \frac{fD}{U}, \tag{2.2}$$

Fig. 2.6 The wake structure of a cylinder in a flowing soap film. The Re number in the experiment is 300

where f is the vortex shedding frequency, D is the diameter of the cylinder, and U is the incoming flow speed. Re number is defined as,

$$Re = \frac{\rho U D}{\mu}, \tag{2.3}$$

where ρ is the fluid density, and μ is the fluid viscosity.

Table 2.1 shows the fitting equations between Re and St in different ranges by different researchers.

Figure 2.7 shows the curves of Eqs. 2.4–2.8 within $47 < Re < 180$. The curves of Eqs. 2.4–2.7 are close to each other. The curve of Eq. 2.8 is away from the rest. This is because Eq. 2.8 fits a large Re range from 70 to 3000. With small Re range in the plot, the displacement becomes obvious. Since the curves of Eqs. 2.4–2.8 are very close, in this thesis, the classic Roshko equation (Eq. 2.4) is selected to calculate the viscosity. According to the relationship between St and Re, the St of a cylinder approaches to 0.2 when Re is greater than 200. In the measurement of viscosity, small diameter cylinders are selected in order to improve the accuracy.

In the practice, a cylinder with diameter of d was inserted in the soap film. A high speed camera was used to record the flow speed U and the wake of the cylinder. By measuring a time-sequenced images, the wake shedding frequency was calculated. St was calculated by Eq. 2.2. Re was calculated by Eq. 2.4. According to the definition of Re in Eq. 2.3, the viscosity of the soap film μ was calculated.

Table 2.2 shows the viscosity of flowing soap film at different flow speeds in both vertical and horizontal soap film tunnels. One thing should be noted is the viscosity of fluid changes with temperature. The viscosity obtained in Table 2.2 was measured at indoor temperature of 10°C.

2.3.2 Surface Tension Coefficient

The soap film flow field is visualized by the interference of lights reflected from its two air–liquid interfaces. The thinner the soap film, the better visualization result can

Table 2.1 Fitting equations between Re and St in different ranges

	Fitting equation	Re range	
Roshko (1954)	$St = 0.212\left(1 - \frac{21.2}{Re}\right)$ $St = 0.212\left(1 - \frac{12.7}{Re}\right)$	$Re < 200$ $Re \geq 200$	(2.4)
Williamson (1988)	$St = 0.1816 - \frac{3.3265}{Re} + 1.600 \times 10^{-4} Re$	$49 < Re < 178$	(2.5)
Williamson and Brown (1998)	$St = 0.2731 - \frac{1.1129}{\sqrt{Re}} + \frac{0.4821}{Re}$	$Re < 1000$	(2.6)
Fey et al. (1998)	$St = 0.2684 - \frac{1.0356}{\sqrt{Re}}$	$47 < Re < 180$	(2.7)
Roushan and Wu (2005)	$St = \frac{1}{5.12 + 313/Re}$	$70 < Re < 3000$	(2.8)

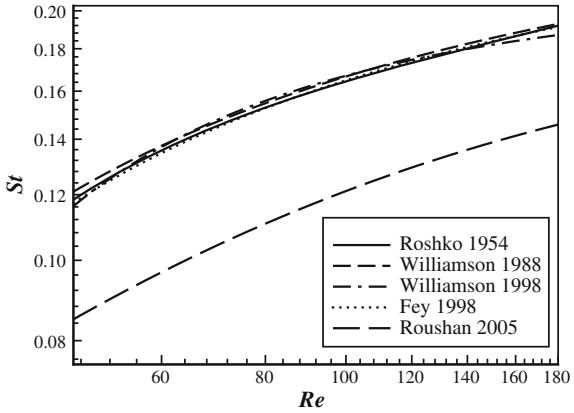

Fig. 2.7 Fitting curves of Re-St relationship

Table 2.2 Viscosity with different flow speed

Device	Flow speed (m/s)	Viscosity μ ($\times 10^{-5}$m^2/s)
Vertical soap film tunnel	1.4	2.00
	1.9	1.22
	2.1	1.20
Horizontal soap film tunnel	0.6	7.75
	0.7	6.74
	0.8	4.90

be achieved. The thickness of a soap film can be maintained depending on its surface tension coefficient. The lower the surface tension is, the thinner the soap film can achieve. By measuring the surface tension coefficient of soap solution with different

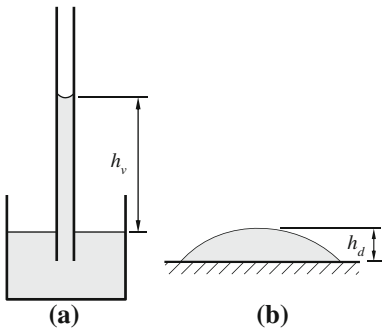

Fig. 2.8 Surface tension measurement methods. **a** Capillary method. **b** Sessile drop method

mixing ratios of water and detergent, we found the ratio for the minimum surface tension coefficient.

Common methods for measuring the surface tension are, Du Noüy Ring method (du Noüy 1919), Du Noüy-Padday method (Tucker et al. 2008), Wilhelmy plate method (Holmberg 2002), Drop volume method, Stalagmometric methods (Somasundaran 2006), Capillary rise method, Bubble pressure method, Pendant drop method, Sessile drop method, Spinning drop method (Rossiter and Baetzold 1993) and so on. Every method has its scope. In this thesis, capillary rise method is selected together with sessile drop method to measure the surface tension coefficient. A simple and convenient measurement is achieved by combining these two methods. Details about the measurement are given here.

Figure 2.8a shows the capillary rise method. By placing a glass tube into the solution, the liquid will rise in the tube due to capillary effect. The liquid is lifted up until its weight is balanced with surface tension. The relationship between the height of the liquid and the surface tension is given by,

$$h_v = \frac{2\gamma_{la}\cos\theta}{\rho g r}, \tag{2.9}$$

where h_v is the vertical height the liquid is lifted, γ_{la} is the surface tension coefficient of the liquid, ρ is the density of the liquid, r is the inner diameter of the glass tube, g is gravity and θ is the contact angle of the liquid on the glass.

According to Eq. 2.9, the contact angle θ is needed when measuring the surface tension coefficient by the capillary rise method. The contact angle can be measured by an expensive contact angle meter. Here we combined the capillary rise method with the sessile drop method, avoiding the measurement of contact angle θ.

Figure 2.8b shows the sessile drop method. By measuring the maximum height of a droplet can maintain on the solid surface, the surface tension can be determined. Here, the solid surface should be the same material as that used in the capillary rise method. The relationship between the height of the droplet and the surface tension coefficient is given by,

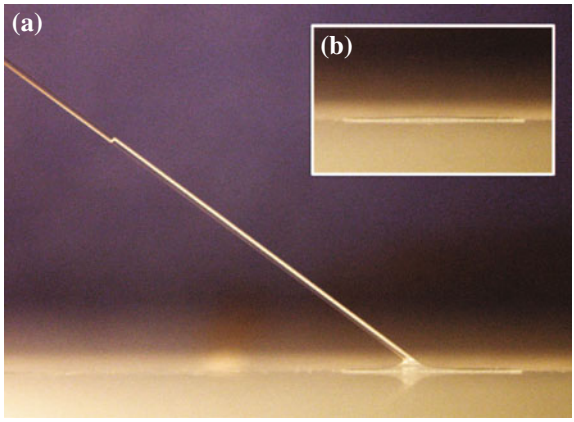

Fig. 2.9 Surface tension measurement. **a** A glass tube is used in the capillary method. The inner diameter of the tube is 0.5 mm. The tube is inclined to get a precise measurement on the raised height of the solution. **b** A glass sheet is used in the sessile drop method

$$h_d = \sqrt{\frac{2\gamma_{la}(1-\cos\theta)}{\rho g}}, \tag{2.10}$$

where h_d is the height of the droplet.

Substituting Eq. 2.9 into 2.10, we get,

$$h_d = \sqrt{\frac{2\gamma_{la}}{\rho g} - h_v r} \tag{2.11}$$

The surface tension γ_{la} is expressed as

$$\gamma_{la} = \frac{1}{2}({h_d}^2 + h_v r)\rho g. \tag{2.12}$$

By measuring the soap solution density, the heights of soap solution in the glass tube and on the glass sheet, the surface tension coefficient is calculated by Eq. 2.12. The soap solution used in experiments were mixture of water, detergent and glycerol. The detergent contains surfactant, which reduced the surface tension of water. Glycerol was used to reduce the evaporation of water, preventing the soap film from broken. In our studies, additive-free household detergent Li Bai was used.

Figure 2.9 shows one photo in the measurement of surface tension coefficient. Figure 2.9a shows the soap solution lifted in the glass tube. The inner diameter of the tube is 0.5 mm. By place the tube inclined, the height of the solution can be measured more precisely. Due to the viscosity of the soap solution, it takes some time for the solution to reach its highest position in the tube. The photo was taken until the liquid did not rise any more. Figure 2.9b is the photo of a droplet on a glass sheet. The heights of the solution in the tube and on the sheet were measured by the photos taken in the measurement. By taking the height into Eq. 2.12, the corresponding surface tension coefficient of the soap solution was calculated.

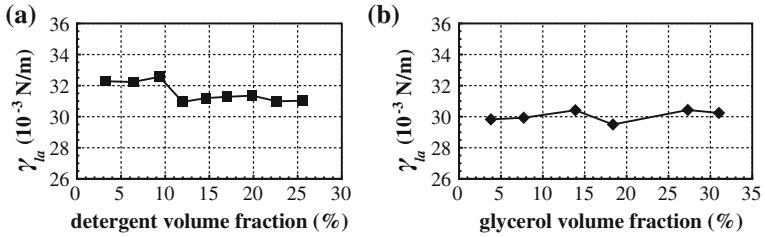

Fig. 2.10 Surface tension coefficient measurement results. **a** The surface tension changing with the detergent volume fraction. **b** The surface tension with different glycerol volume fraction

The result of surface tension coefficient is shown in Fig. 2.10. Figure 2.10a shows the change of surface tension coefficient with different volume fraction of the detergent, without adding of glycerol. We can see, the surface tension coefficient changes little after the detergent concentration is more than 12 %. Figure 2.10b shows the change of surface tension coefficient by adding glycerol into the solution. The detergent concentration is fixed at 12 %. We can see the surface tension coefficient of the soap solution keeps no change with adding glycerol in it. It seems the glycerol has little effect on reducing the surface tension coefficient. However, once the soap solution becomes soap film, its surface area is greatly increased. The evaporation cannot be ignored. Due to the evaporation, the thickness of the soap film reduces and the soap film becomes easy to break. By adding glycerol into the solution, it helps to reduce the evaporation, and maintains the soap film for a longer time. In our experiments, 5 % glycerol is added into the soap solution.

2.3.3 Flow Velocity

Soap film flow speed is an important experimental parameter for soap film tunnels. Only accurate flow speed can determine the dimensionless flow parameters, such as Reynolds number, Strouhal number.

The flow speed of soap film can be determined by Laser Doppler Velocimetry (LDV). It measures the speed of flowing soap film at one point. If multi-points measurement is needed, the LDV device is required to move. The laser of LDV needs to be focused on the soap film during the velocity measurement. The soap film is very thin, adjusting the position of LDV usually leads the laser to focus out of the film, resulting in a failure of velocity measurement. Particle Image Velocimetry (PIV) is another common device for measuring flow velocity. By seeding tiny particles into flow, PIV can track the movement of the particles. The particles are moving together with flow at the same speed. Thus, PIV can measure the flow speed. Due to the soap film being very thin, commonly used tracking particle with diameter above 5 μm does not fulfil the requirement for the particle density per unit area. If too many particles are added into the soap solution, they will block the flux control valve.

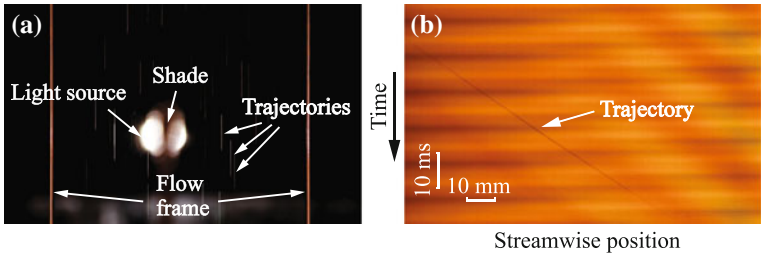

Fig. 2.11 Soap film flow speed measurement. **a** Single fixed time exposure velocimetry. **b** Tracking the motion of defects in the soap film

Rutgers et al. (2001) proposed to use titanium dioxide ultrafine powder as tracking particles. However, the use of ultrafine powder arises some difficulty in illumination.

The flow speed of the flowing soap film generated by the soap film tunnels is very stable. With a given flow flux, the film speed is constant. It allows us to measure the flow speed in different positions at different time. In our studies, two simple methods are introduced to measure the flow speed.

(a) Single fixed time exposure velocimetry

This is a simplified method of Particle Tracking Velocimetry (PTV). It uses fewer particles compared to the PIV method used. As a result, it measures velocities of fewer locations than PIV does. A small amount of tracking particles are added to the soap solution. Light source is placed behind the film. Diffraction occurs when light is projected to the moving particles in the soap film. A camera is placed in front of the soap film. It records the trajectories of particles at a fixed exposure time as shown in Fig. 2.11a. By measuring the lengths of the particles' trajectories, and dividing them with the exposure time, we get the velocities in the flow field where the particles are located. During the measurement, an appropriately sized shade should be placed in the optical path between the light source and the camera, blocking any light from directly projecting into the camera, in order to avoid any overexposure.

(b) Tracking the motion of defects in the soap film

After a long-time exposing to air, the soap solution is inevitably mixed with some dusts. The dusts running in the soap film are visualized as defects in the interference fringes. By recording and tracking the motion of the defects, the flow speed can be determined. Figure 2.11b shows the trajectory of a defect over time. In the plot, the horizontal direction is flow direction, and the vertical direction is time advancing direction. By combining a series of slices from a time-sequenced high speed camera recorded images, we get the defect's track over time. The plot in Fig. 2.11b is similar to the image recorded by a streak camera. A clear slash can be read from Fig. 2.11b. Its slope corresponds to flow speed. In the figure, the angle of the slash to the horizontal is 33.9°. Its corresponding flow speed is 1.9 m/s.

Table 2.3 Linear density of the filament

Condition (L=21.2 cm)	Mass (mg)	Linear density (kg/m)
Dry	0.96	4.5×10^{-6}
Wet	2.68	1.3×10^{-5}

In our experiments, the vertical soap film tunnel achieves a steady flow speed ranging from 1.3 to 2.1 m/s and the horizontal soap film tunnel ranging from 0.9 to 1.5 m/s.

2.4 Physical Properties of Filaments

In our studies, flexible filaments play the role of flexible plates. A filament consists of a bulk of silk threads. The measurement methods of its physical properties are introduced as follows.

2.4.1 Linear Density

The linear density of the filament is extremely small. In the measurement, we measured a long filament using an analytical balance with accuracy of 0.1 mg (TG328B, Shanghai Tianping Instrument Technology Co. LTD). The linear density was obtained by dividing the mass with its length. The filament consists of a bulk of silk threads. Space exits between silk threads. In the experiments, the space was filled with soap solution. The solution moved as a part of the filament. Here, we measured the linear density of the filament in dry and wet. In order to avoid the evaporation of soap solution, plastic wrap was wrapped around the wetted filament in the measurement of wet soap filament. Table 2.3 shows the result.

2.4.2 Bending Stiffness

By measuring the displacement of a filament with a known force, its bending stiffness can be determined. For a filament with one end clamped and the other end applied with a known tiny force, its displacement can be determined by the equation of a clamped beam, expressed as following,

$$y = \frac{pL^3}{3EI}, \tag{2.13}$$

where y is the displacement at the end, p is the applied force, L is the length of the filament, and EI is the bending stiffness.

By measuring the displacement of filament with a known force, its bending stiffness can be determined. Since the flexural rigidity of the filament is small, the corresponding load applied on its end should be small too. In the practice, we used uniform density wire with diameter of 50 μm. Different lengths of wire were used as different loads. The deflection of the filament is measured from images taken in the measurement. The bending stiffness is calculated by Eq. 2.13. The result shows the bending stiffness of the filament $EI = 6.2 \times 10^{-10}\,\mathrm{N\,m^2}$.

2.5 Summary

In this chapter, the experimental apparatus and parameters measurement methods are introduced.

The details of vertical and horizontal soap film tunnels are given. The designs are based and improved from previous research works. These two devices provide uniform and stable soap film, which is an ideal tool to carry out two-dimensional fluid dynamics experiments. The experimental studies discussed in this thesis were carried out using these two devices.

Interferometry is used to visualize the flow structure in the soap film. The interference fringes which reflect the flow structure are recorded by camera and high speed camera. In order to record the interference fringes, special requirement is needed for the lighting device. The design of lighting device is also introduced in this chapter.

In this chapter, the measurement methods and results of the soap film flow parameters and physical properties of the filaments are also given. These physical parameters are the basic parameters in the experiments of flapping filaments in a two-dimensional flowing soap film.

References

Chomaz JM (2001) The dynamics of a viscous soap film with soluble surfactant. J Fluid Mech 442:387–409

Fey U, König M, Eckelmann H (1998) A new strouhal-reynolds-number relationship for the circular cylinder in the range 47. Phys Fluids 10:1547–1549

Georgiev D, Vorobieff P (2002) The slowest soap film tunnel in the southwest. Rev Sci Instrum 73(3):1177–1184

Greco V, Molesini G (1996) Monitoring the thickness of soap films by polarization homodyne interferometry. Meas Sci Technol 7(1):96–101

Holmberg K (2002) Handbook of applied surface and colloid chemistry. Wiley, New York

Martin B, Wu XL (1995) Shear flow in a two-dimensional couette cell: a technique for measuring the viscosity of free-standing liquid films. Rev Sci Instrum 66(12):5603–5608

du Noüy PL (1919) A new apparatus for measuring surface tension. J Gen Physiol 1(5):521–524

Roshko A (1954) On the development of turbulent wakes from vortex streets. Technical report, National Advisory Committee for Aeronautics

Rossiter BW, Baetzold RC (1993) Investigations of surfaces and interfaces-Part A, 2nd edn. Wiley, New York

Roushan P, Wu X (2005), Structure-based interpretation of the strouhal-reynolds number relationship. Phys Rev Lett 94(5):054, 504

Rutgers MA, Wu X, Daniel WB (2001) Conducting fluid dynamics experiments with vertically falling soap films. Rev Sci Instrum 72(7):3025–3037

Sakurambo (2006) Diagram of a high pressure sodium vapor lamp. http://en.wikipedia.org/wiki/File:High_pressure_sodium_lamp.svg

Settles GS (2001) Schlieren and shadowgraph techniques: visualizing phenomena in transparent media. Springer, Berlin

Somasundaran P (2006) Encyclopedia of surface and colloid science, 2nd edn. Taylor & Francis, London

Trapeznikov AA (1957) Application of the method of two-dimensional viscosity and shear strength to the investigation of the structure and composition of two-sided films and surface layers in solutions of soaps and saponins. In: Proceeding of 2nd international congress on surface activity, pp 242–258

Tucker C, Mohler C, Harris K (2008) High throughput surfactant synthesis, characterization and formulation. SÖFW-J 134(9):80–90

Williamson CHK (1988) Defining a universal and continuous strouhal-reynolds number relationship for the laminar vortex shedding of a circular cylinder. Phys Fluids 31(10):2742–2744

Williamson CHK, Brown GL (1998) A series in $1/\sqrt{Re}$ to represent the strouhal-reynolds number relationship of the cylinder wake. J Fluids Struct 12(8):1073–1085

http://www.springer.com/978-3-662-43674-5

The Interaction Between Flexible Plates and Fluid in Two-dimensional Flow

Jia, L.

2014, XVII, 103 p. 57 illus., 23 illus. in color., Hardcover
ISBN: 978-3-662-43674-5